

SUPPLEMENTAL METHODS

Sample collection and selection

Samples were collected from patients undergoing breast surgeries at the McGill University Health Centre (MUHC) between 1999 and 2012 who provided written, informed consent (MUHC REB protocols SDR-99-780 and SDR-00-966). All tissues were snap-frozen in O.C.T. Tissue-Tek Compound (#4583 from Sakura Finetek Europe B.V. KvK) within 30 minutes of removal. For the purposes of this study, samples were selected according to the following criteria: therapy-naïve at time of surgical excision, clinically documented lack of expression/amplification of ER, PR and HER2, a histological subtype assignment of invasive ductal carcinoma (not otherwise specified) (IDC (NOS)) and availability of matched formalin-fixed paraffin-embedded (FFPE) tumor blocks. Information regarding clinical variables and disease course (follow-up) was obtained through review of Medical Records at the MUHC. 5µm sections from frozen tissue were prepared for each sample, subjected to routine haematoxylin and eosin (H&E) staining, and evaluated by an attending clinical pathologist with expertise in breast tissue to identify invasive, in situ and normal components. Subsequently, additional frozen sections were sectioned at 10 µm thickness, stained using the HistoGene kit (Life Sciences) and subjected to laser capture microdissection on an Arcturus PixCell Ile system (Molecular Devices) to isolate epithelial and non-epithelial (stromal) compartments of the tumor bed as identified above, avoiding lymphocyte-dominant regions within the non-epithelial compartment. All microdissections were performed within three hours of tissue staining. Total RNA was extracted from each population of microdissected cells using the Arcturus PicoPure RNA Isolation Kit (Life Technologies; Cat. No. 12204-01). Following extraction, total RNA yield and quality was assessed using a 2100 Bioanalyzer (Agilent Technologies). For samples exhibiting distinct 28S and 18S rRNA peaks, between 100 pg and 5 ng of total RNA were then subjected to two rounds of T7 linear amplification using the Arcturus® RiboAmp® HS PLUS Kit (Life Technologies; Cat. No. KIT0525) and labeled with Cy3 dye (Arcturus® Cy3 Turbo Labeling™ Kit, Life Technologies; Cat. No. KIT0609)

according to the manufacturer's protocol. Hybridizations were performed using a common reference design. The common reference used for all arrays was Universal Human Reference RNA (Stratagene, Cat. No. #740000), subjected to two rounds of T7 linear amplification using the Arcturus® RiboAmp® HS PLUS Kit and labeled with Cy5 dye (Arcturus® Cy3 Turbo Labeling™ Kit) according to the manufacturer's protocol. Prior to microarray hybridizations, amplified products were quantified using a spectrophotometer (NanoDrop) and subjected to BioAnalyzer assays (Agilent Technologies) for quality control. Agilent Technologies SurePrint G3 Human GE 8x60K Microarrays (Cat No G4851A) were used for all experiments. Amplified RNA samples (300 ng) were subjected to fragmentation followed by 17h of hybridization, washing, and scanning (Agilent G2505C scanner, Agilent Technologies) according to the manufacturer's protocol (manual G4140-90050). Cy3-labeled samples were hybridized against Cy5-labeled reference for all arrays. Microarray data were feature-extracted using Agilent Feature Extraction Software (v. 10.7.3.1) with the default parameters.

Pathway analyses, signature score and development of Metasignatures

Analysis for the enrichment of publicly available. All pathways related to TGF β signaling were extracted and used as gene sets for the enrichment analysis. We performed gene set enrichment analysis (GSEA) using the *Piano* R package (version 1.12.0). Nominal *P* values obtained for each pathway are corrected for multiple testing using the false discovery approach (FDR). For representation as a heatmap, we calculated single-sample gene set enrichment score, using the GSVA R package (version 1.20.0) to derive the absolute enrichment scores of the significant (FDR<0.05 by GSEA) previously experimentally derived TGF β gene signatures. TGF β signature single sample enrichment scores were clustered by Pearson dissimilarity (1-cor) distance using Ward clustering as the agglomeration method.

Immunohistochemistry (IHC) and immunohistochemistry (IHF)

Table of primary antibodies used in this study

Ab Target	Clone	Reference	Company	Dilution	Application	Antigen retrieval	TSA used for IHF
B7-H4	D1M8I	14572	Cell Signaling	1/200	IHF	Citrate	yes
CD206	-	ab64693	Abcam	1/1000	IHF	Citrate	yes
CD4	4B12	M7310	Ventana	1/50	IHF	EDTA	
CD68	KP-1	790-2931	Ventana	1/3	IHF	Citrate	yes
CD8a	C8/144B	M710301-2	DAKO	1/50	IHC/IHF	Citrate	no
FoxP3	-	NBP2-32001	Novus	1/300	IHF	EDTA	
Granzyme B	GrB-7	NBP1-51746	Novus	1/50	IHF	EDTA	yes
HLA-ABC	EMR8-5	ab70328	Abcam	1/100	IHC	Proprietary	-
IDO-1	-	ab228468	Abcam	1/100	IHF	EDTA	
IL-17F	-	AF1335	R&D biosystems	1/50	IHF	Citrate	yes
Neutrophil Elastase	SP203	760-4953	Ventana	1	IHC	Proprietary	-
Pan-cytokeratin	AE1/AE3 & PCK26	760-2135	Ventana	1/2	IHF	Citrate	no
PD-L1	SP142	M4422	Spring Bioscience	1/100	IHF	Citrate	yes

IHC protocol.

IHC directed against HLA-ABC and neutrophil elastase was performed on a Ventana Benchmark XT automated system. Subsequent steps were performed as per the manufacturer's directions. Other IHC procedures were performed manually as follows. Sections were deparaffinized, conditioned and antigens were retrieved using proprietary buffers (pH6 or pH9) (from Vector Laboratories, #H-3000 and #H-3301, respectively,). Slides were blocked for 5 minutes with Power Block reagent (Universal Blocking Agent (Power Block) Biogenics CAT# HK085-5K). Primary antibodies were applied at optimized concentrations overnight at 4°C, followed by 30 minutes of incubation with SignalStain Boost (Cell Signaling #8114 or #8125). Detection was performed with a DAB substrate kit (Cell Signaling #8059). Slides were counterstained with Harris Haematoxylin.

IHF protocol. Sections were deparaffinized, conditioned and antigens were retrieved using proprietary buffers (pH6 or pH9) (from Vector Laboratories, #H-3000 and #H-3301, respectively). Slides were blocked for 5 minutes with Power Block reagent. Primary antibodies were applied at optimized

concentrations overnight at 4°C, followed by 30 minutes of incubation with SignalStain Boost (Cell Signaling). Detection was performed with Tyramide Signal Amplification (TSA) kits (Thermo Fisher Scientific). Slides were counterstained with DAPI.

IHC and IHF quantification

IHC for CD8⁺ T cells (anti-CD8) and neutrophils (anti-neutrophil elastase). Complete IHC-stained sections were digitally acquired using an Aperio ScanScope XT slide scanner (Leica Biosystems) at 20X or 40X magnification. CD8⁺ T cell (CD8A) and Neutrophils (NE) quantification was performed using a customized version of the *Positive Pixel Count v9* algorithm (Leica Biosystems) via a Spectrum database system (Leica Biosystems). Tumor margins, core, stroma and epithelium were manually annotated. For tumor margin areas, a region spanning 250µm on either side of the margin *per se* was annotated (total width, 500µm). For the tumor core, all regions inside the area considered to be tumor margin were analyzed, except regions of necrosis, staining artefacts and folds. For the tumor stroma and tumor epithelium, regions were manually annotated; only regions lying within the tumor core were considered. A total area of >1mm² was analyzed for each compartment within each sample unless otherwise specified. One cell was determined to correspond to 250 strong positive pixels (SPP) as determined by the *Positive Pixel Count v9* algorithm (CD8⁺ cell count = SPP/250).

IHF for IL-17 producing cells, macrophages and immunosuppression markers on internal LCM cohort n=38 TNBC. Images of the IHF-stained sections were acquired at 20X and 40X using the LSM800 (Carl Zeiss Canada) confocal imaging system. Combinations of antibodies were: IL-17 producing cells: IL-17F, pan-cytokeratin/PanCK; Macrophages: CD68, CD206, PanCK; Immunosuppression markers: PD-L1 and B7-H4. IHF sections stained for IDO1 were scanned with an AxioScan Z1 slide scanner (Carl Zeiss Canada). IL-17F-producing cells were counted manually on 3 images of 0.1mm² each per tumor. The quantification of the area of tumor stroma and epithelium per image was

performed using the classifier of the HALO™ software package (Indica Labs) based on PanCK staining. Macrophages were quantified using the “Cytonuclear analysis” module from the HALO™ software package (Indica Labs) after stromal/epithelial classification based on PanCK staining on 2 images of 0.37 mm² each per tumor. Immunosuppression markers were analyzed using the “Area quantification” module from the HALO™ software package after manual identification of stromal and epithelial tumor compartments based on DAPI staining. Quantification was performed on 3 images of 0.1mm² each per tumor.

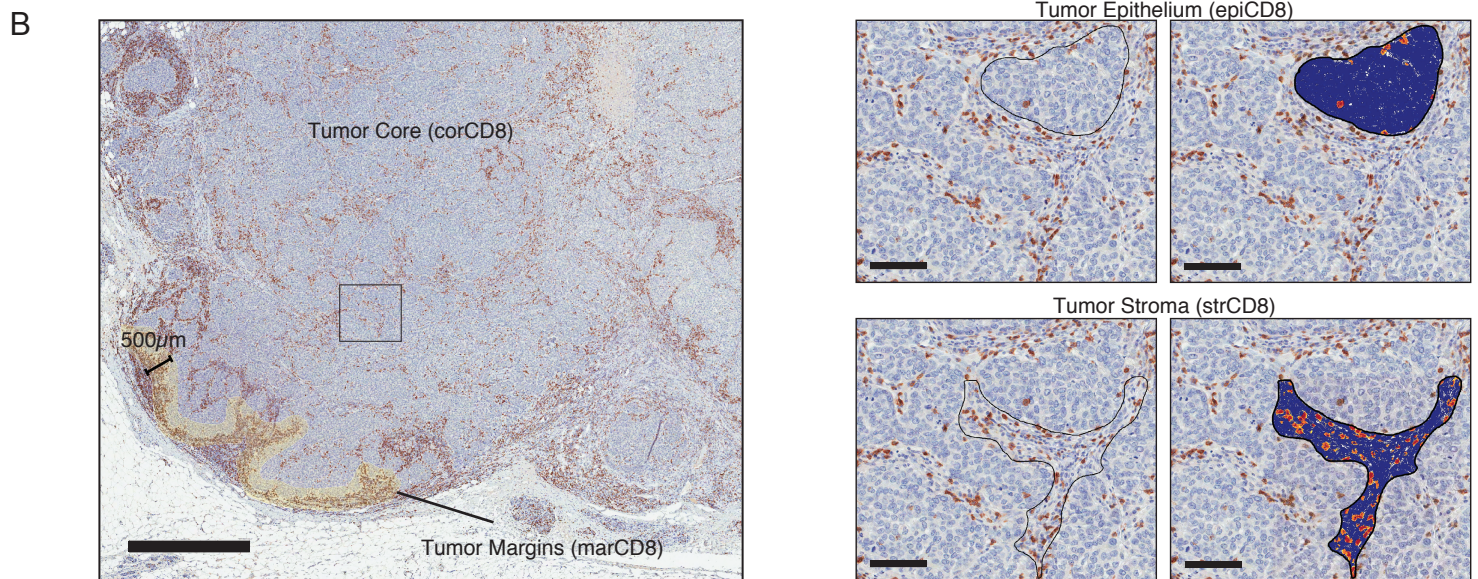
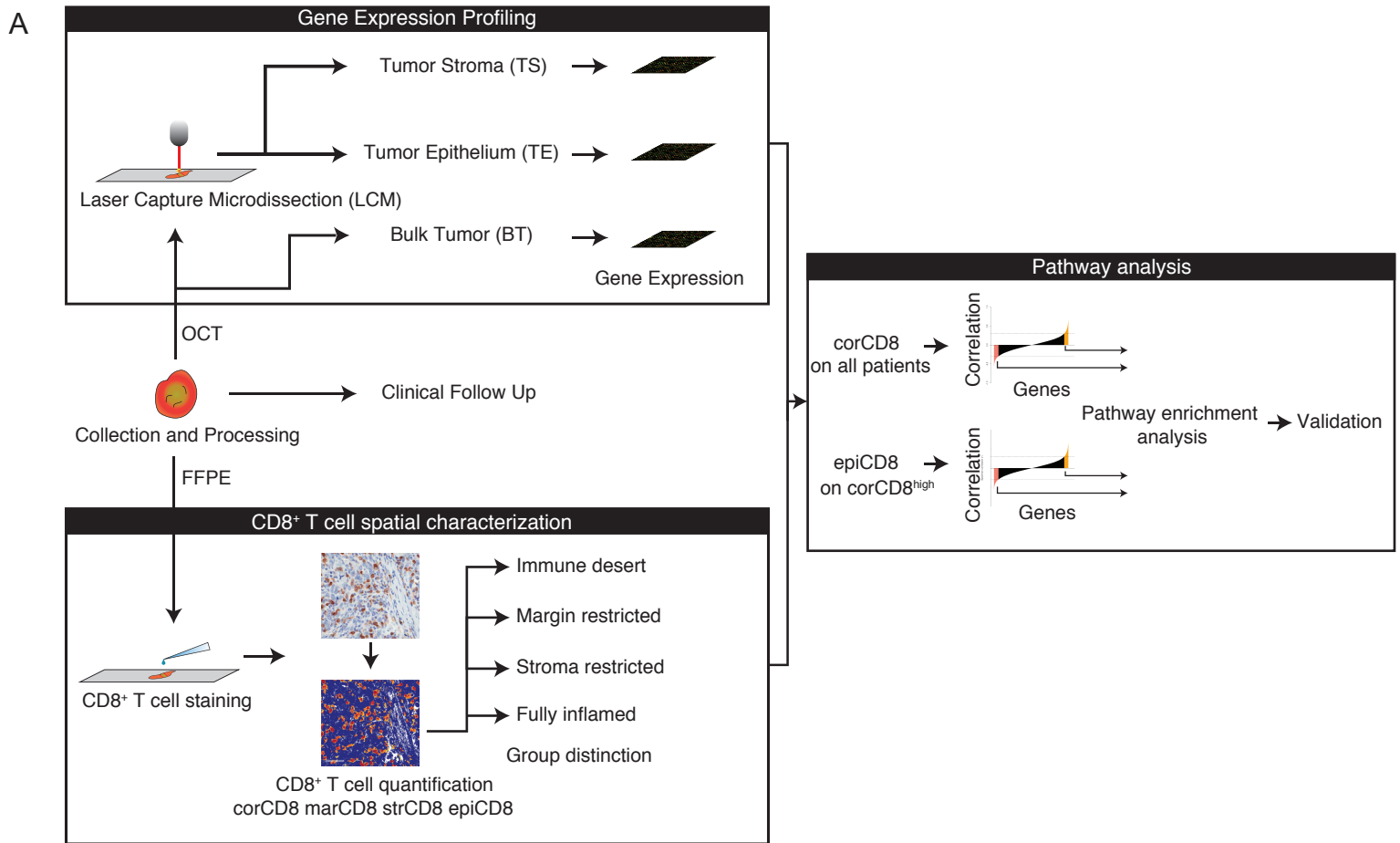
IHF for GranzymeB expressing (GzmB⁺) CD8⁺ T cells. IHF-stained sections were scanned with an AxioScan Z1 slide scanner (Carl Zeiss Canada). Scans were annotated as follows. Necrotic regions, tissue folds, edge effects and fluorescence artefacts were manually excluded. Based on PanCK staining, the limits of the tumor and juxtatumoral tissue was automatically determined and then manually adjusted. The tumor core is defined as the area within the tumor border lying at least 250 μm away from the tumor limit. In the tumor core, between 2 and 9 representative regions were selected to run the quantification algorithm depending on tumor size and annotations determined. CD8⁺ GzmB⁺ T cells were quantified using the Cytonuclear analysis module from HALO™ software (Indica Lab) after stroma/epithelium classification based on PanCK. Each selected region was visually assessed for correct performance of the quantification algorithm.

IHF for CD4⁺ FoxP3⁺ T cells. IHF-stained sections were scanned with an AxioScan Z1 slide scanner (Carl Zeiss Canada). Scans were annotated as follows. Necrotic regions, tissue folds, edge effects and fluorescence artefacts were manually excluded. Based on PanCK staining, the limits of the tumor and juxtatumoral tissue was automatically determined and then manually adjusted. CD4⁺ FoxP3⁺ T cells were quantified using the Cytonuclear analysis module from HALO™ software (Indica Lab) after stroma/epithelium classification based on PanCK. Each selected region was visually assessed for correct performance of the quantification algorithm.

Pathological assessment

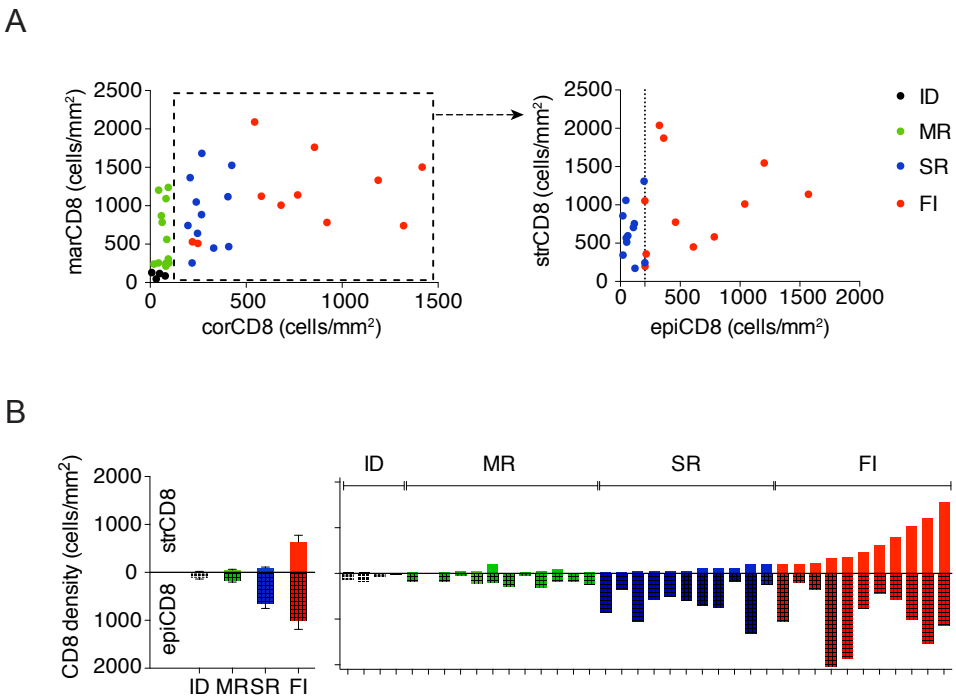
Scoring of tumor infiltrating lymphocytes (TILs) on H&E sections was performed by two trained pathologists (R.S., G.V.d.E.) who were blinded to the clinical and experimental data. TIL infiltration was assessed as a continuous variable based on the percentage of tissue area occupied by TILs. Lymphocytes in direct contact with tumor cells were identified as intratumoral TIL (iTILs) and those in the stroma (within the borders of the invasive carcinoma or its immediate surroundings) as stromal TILs following the proposed guidelines for breast cancer (8). The evaluation of fibrotic focus on H&E sections was also performed by two trained pathologists (R.S., G.V.d.E.) who were blinded to the clinical and experimental data. Presence of fibrotic foci was determined by the presence of an area of exaggerated reactive tumor stroma formation as per the proposed guidelines(16).

Supplemental Figure 1



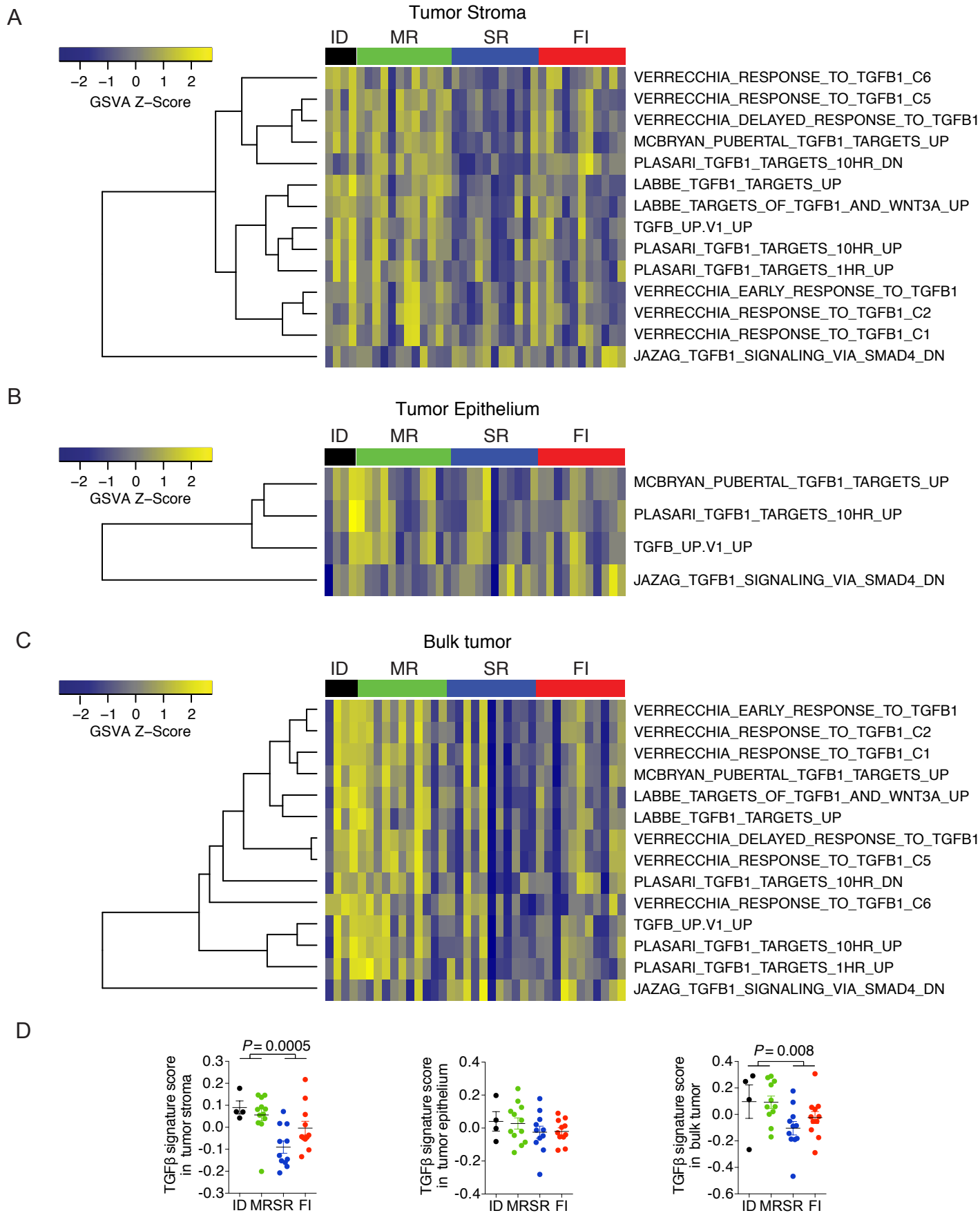
Supplemental Figure 1. Study workflow and CD8⁺ T cell quantification methodology. A) Study workflow; frozen samples of therapy-naive primary TNBC tumors were subjected to laser capture microdissection (LCM) to isolate tumor stroma and epithelium. RNA was isolated from each compartment, as well as from undissected sections of bulk tumor, and subjected to gene expression analysis. Separately, Formalin-fixed paraffin-embedded (FFPE) samples from the same matched patients were stained for CD8 by immunohistochemistry (IHC). CD8⁺ T cell density was then quantified at tumor margins (marCD8) and within tumor core (corCD8), tumor stroma (strCD8) and tumor epithelium (epiCD8). Based on these 4 factors, each tumor was assigned to a group depending on CD8⁺ T cell localization in the tissue. Group assignments and CD8⁺ T cell density values were used for analysis of the gene expression data collected. n=38. B) Examples of the CD8⁺ T cell quantification on IHC. Left, representative image of whole tumor sections stained for CD8 by IHC. Tumor margin (defined as 250 μm inside + 250 μm outside the tumor boundary, highlighted in yellow) and tumor core areas are indicated. Small rectangle indicates the region zoom depicted on the right. Scale 1mm. Right, representative section of tumor stroma and tumor epithelium quantified for CD8⁺ T cell density before (left) and after (right) application of algorithm. Regions of CD8⁺ T cell positivity are depicted by strong positive pixels (red). Scale 100μm.

Supplemental Figure 2



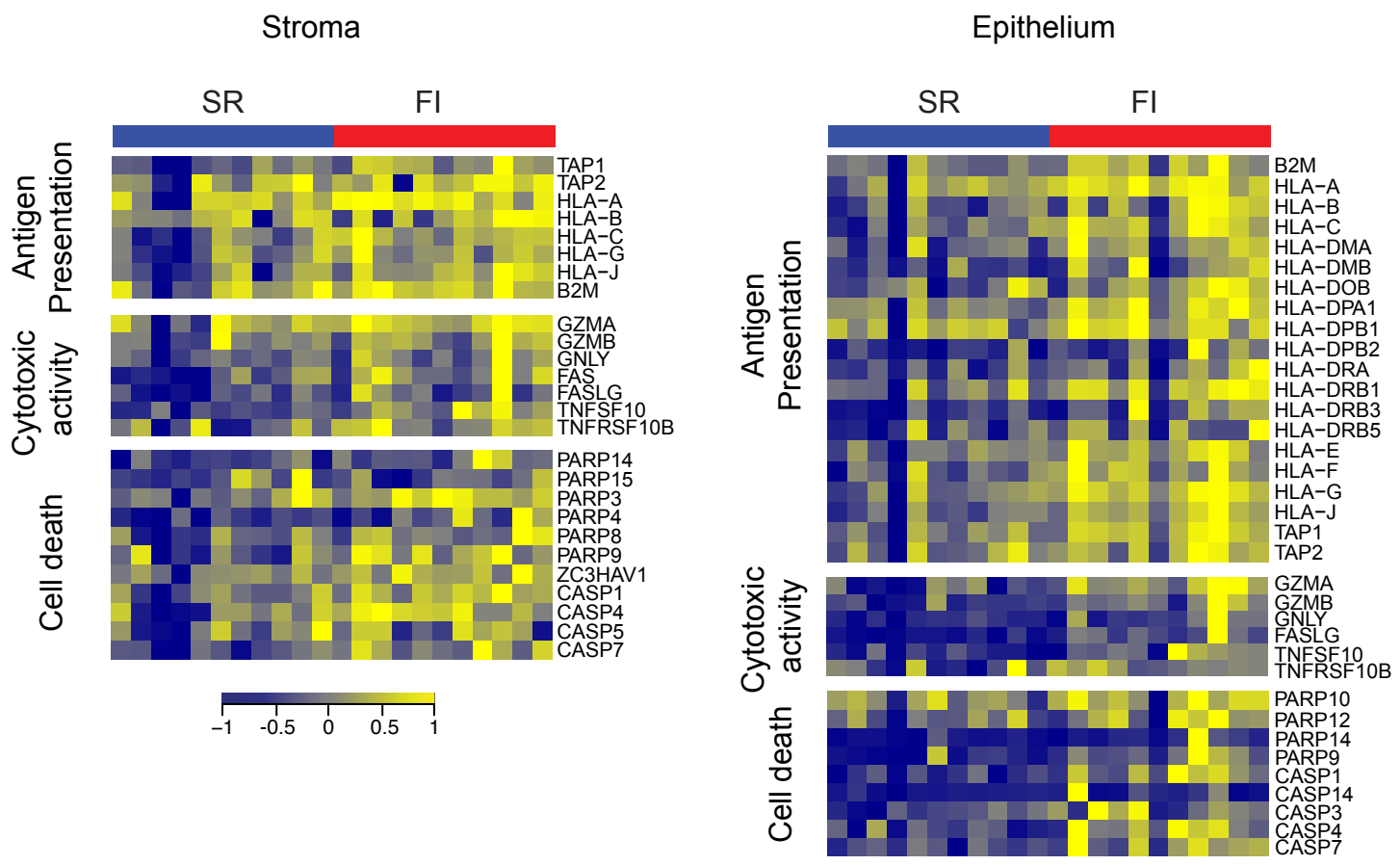
Supplemental figure 2. CD8⁺ T cell quantification on our cohort of 38 therapy-naïve TNBC tumors. A) Left, quantification of CD8⁺ T cell densities at tumor margins (marCD8) and core (corCD8) (n=38). Right, quantification of CD8⁺ T cells in the tumor stroma (strCD8) and epithelium (epiCD8) for the tumors showing significant infiltration of CD8⁺ T cells in the tumor core (corCD8^{high}; dotted square) (n=38). Dotted line represents the median. B) CD8⁺ T cell densities in tumor epithelium (epiCD8) and stroma (strCD8) of individual tumors (right) and the mean per group (left) (n=38). Black, green, blue and red represent ID, MR, SR and FI tumors respectively. Error bars, mean ± SEM.

Supplemental Figure 3



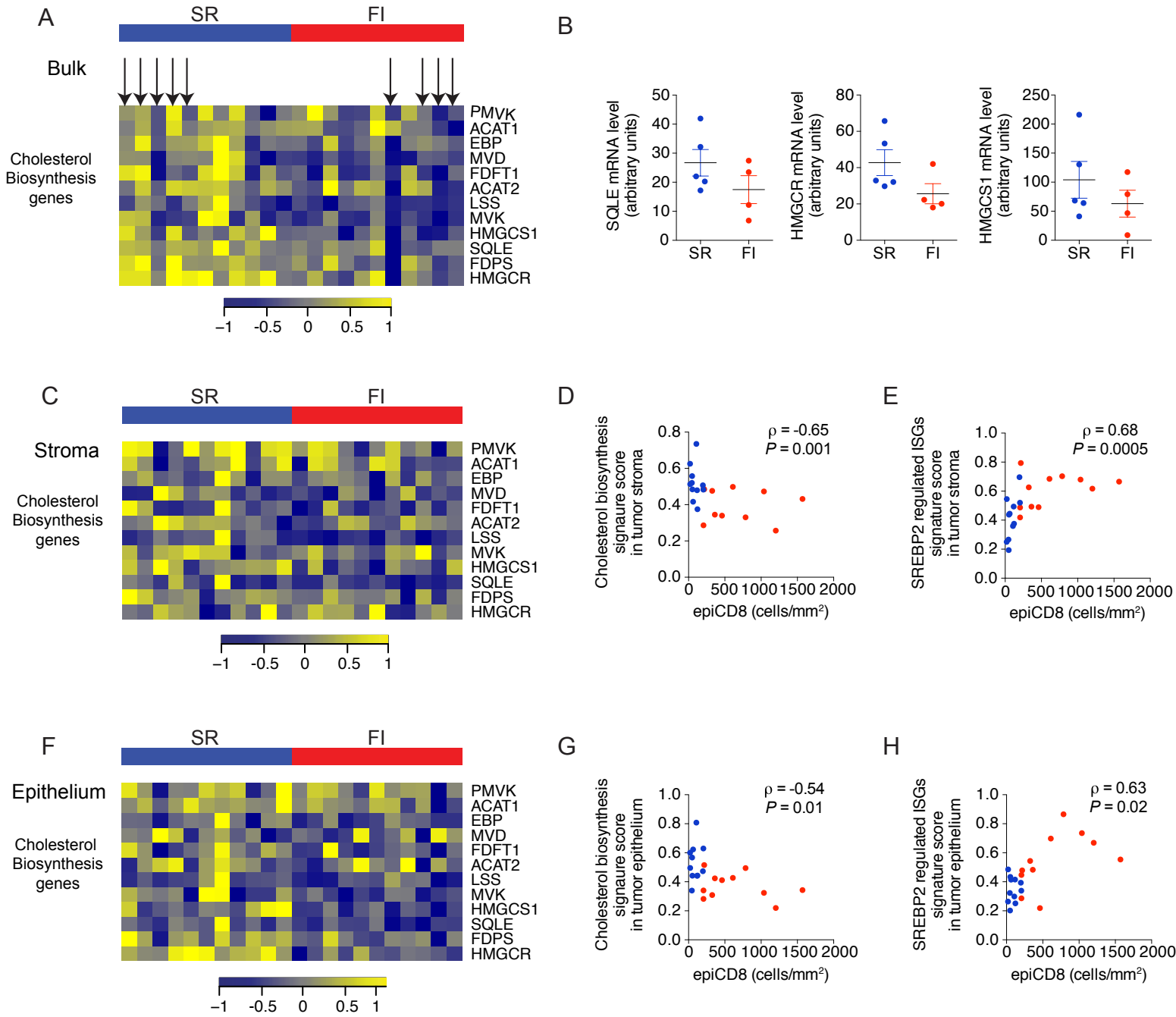
Supplemental Figure 3. Gene set enrichment analysis (GSEA) for genes positively or inversely correlated with CD8⁺ T cell core density (*corCD8*) using publicly available TGFβ signatures from MSigDB C2 (Curated gene sets) and C6 (Oncogenic signatures) subset reveals a significant representation of TGFβ signalling in the stroma of tumors devoid of CD8⁺ T cell infiltration (*corCD8*^{low}, IC and MR). A-C) Heatmaps showing GSVA scores for the TGFβ pathways considered significant by GSEA (FDR < 0.05) in tumor stroma (n=38) (A), tumor epithelium (n=38) (B) and bulk tumor (n=37) (C). D) Signature score of genes present in the pathways depicted in heatmap (A) for tumor stroma (n=38), in heatmap (B) for tumor epithelium (n=38) and in heatmap (C) for bulk tumor (n=37) as indicated. Mann-Whitney test. Error bars, mean±SEM. Black, green, blue and red represent ID, MR, SR and FI, respectively.

Supplemental Figure 4



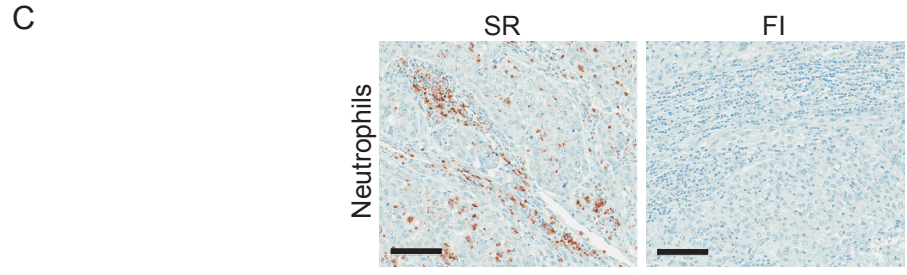
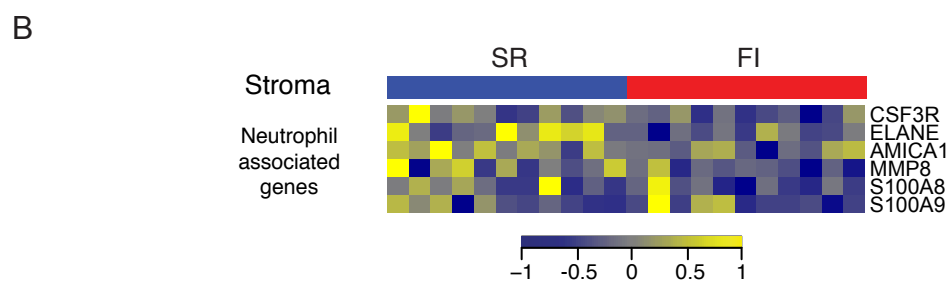
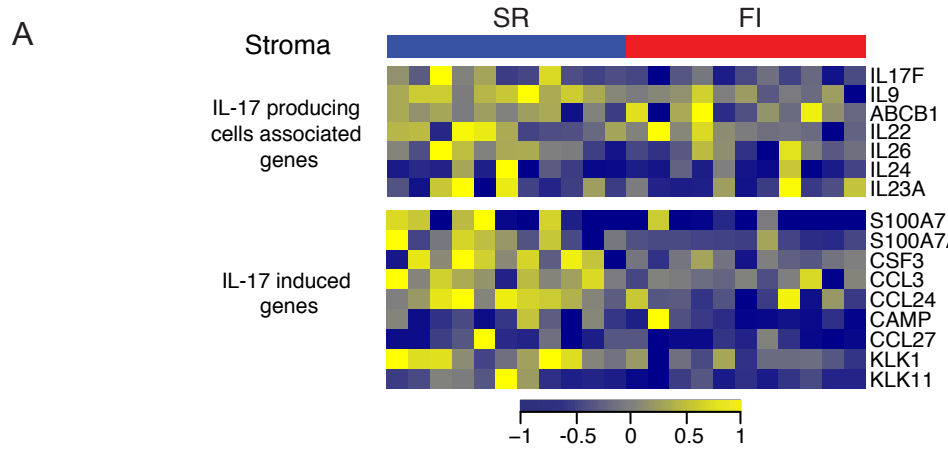
Supplemental Figure 4. Heatmaps depicting expression of genes associated with antigen presentation, cytotoxic activity and cell death in the tumor stroma and epithelium in SR and FI TNBC (n=22).

Supplemental Figure 5



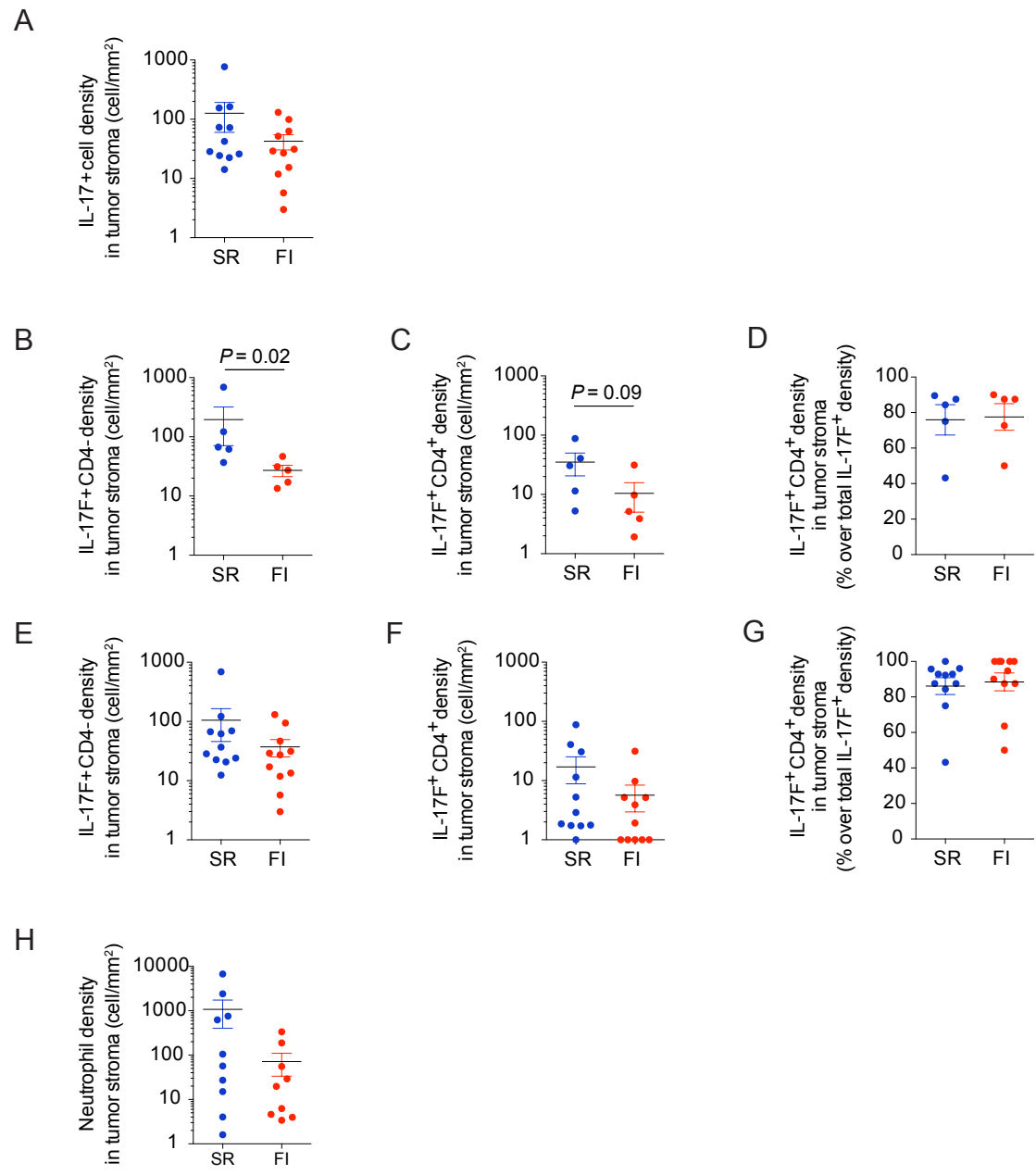
Supplemental Figure 5. Tumors with CD8⁺ T cell accumulation in the tumor stroma are defined by a cholesterol gene expression signature. A-B) Heatmap depicting expression of genes associated with the superpathway of Cholesterol biosynthesis in bulk tumor (n=22). Arrows represent the tumors for which qPCR was performed in (B); for SQLE, HMGCR, HMGCS1 accordingly. C) Heatmap depicting expression of genes associated with the superpathway of Cholesterol biosynthesis in tumor stroma (n=22). D) Signature score of genes depicted in (C). Spearman correlation. Stat and FDR values from Figure 2 are Stat=-0.56, P=0.02. E) Signature score of Interferon Stimulated Genes (ISGs) repressed by SREBP2 showing decreased expression in tumor stroma for SR compared to FI tumors (n=22). Spearman correlation. F) Heatmap depicting expression of genes associated with the superpathway of Cholesterol biosynthesis in tumor epithelium (n=22). G) Signature score of genes depicted in (F). Spearman correlation. Stat and FDR values from Figure 2 are Stat=-0.43, P=0.28. H) Signature score of Interferon Stimulated Genes (ISGs) repressed by SREBP2 showing decreased expression in tumor epithelium for SR compared to FI tumors (n=22). Spearman correlation. Stroma restricted (SR) are depicted in blue and Fully inflamed (FI) in red.

Supplemental Figure 6



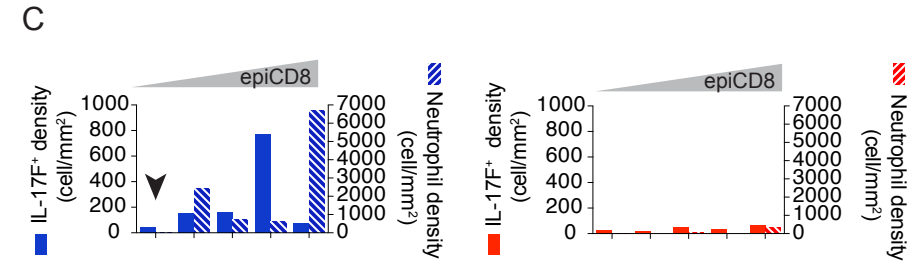
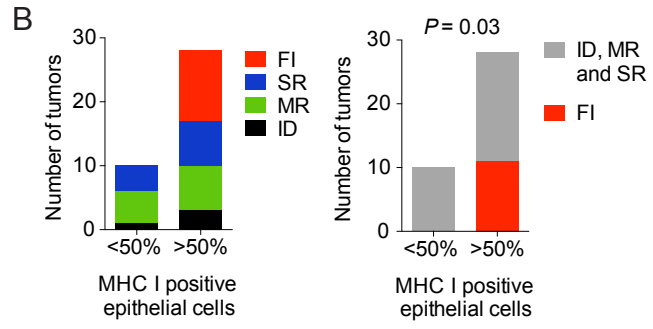
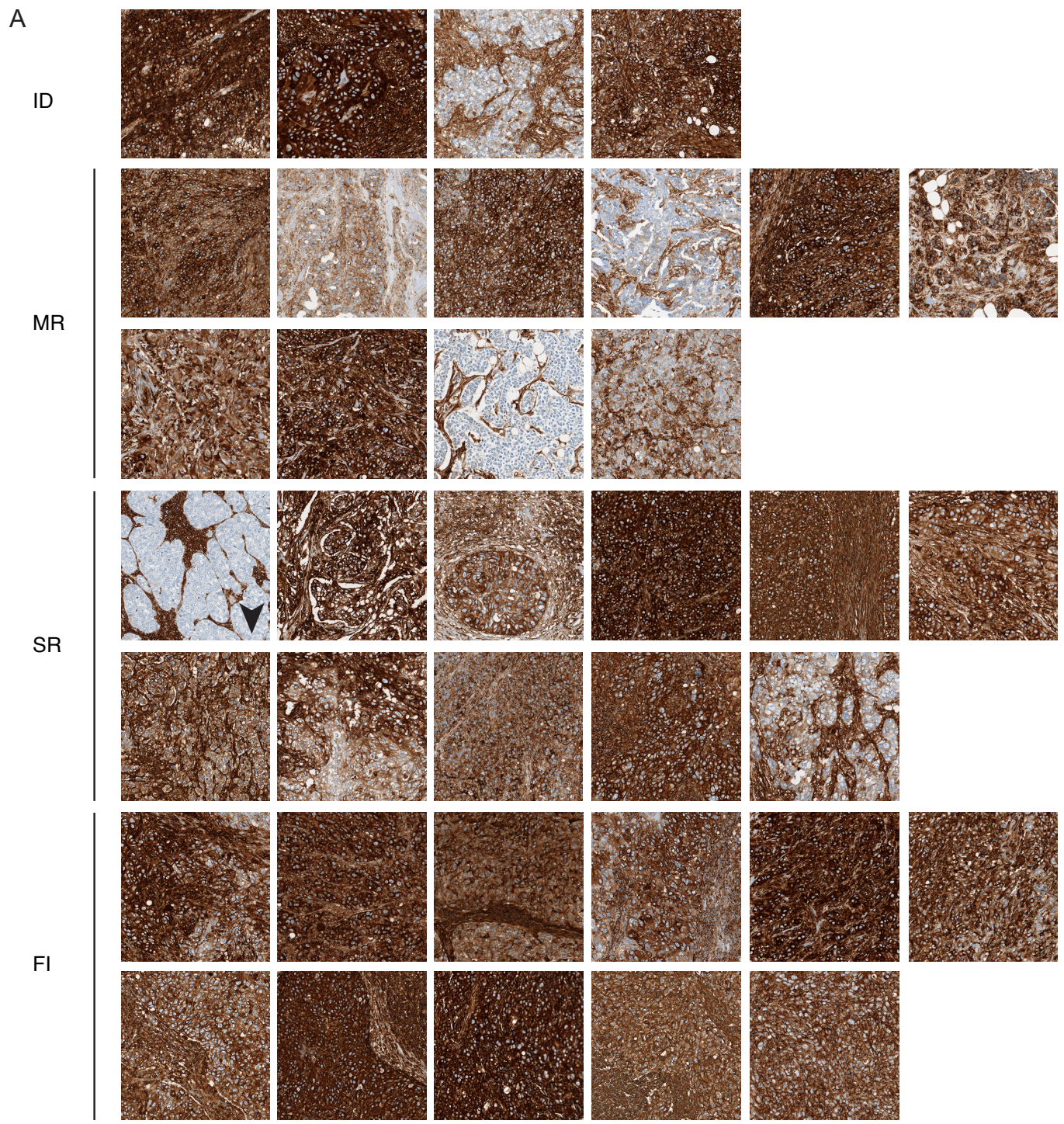
Supplemental Figure 6. Stroma restricted tumors display a distinct TIME. A) Heatmap depicting increased expression of genes associated with IL-17-producing cells and IL-17 exposure in tumor stroma of SR compared to FI tumors (n=22). B) Heatmap depicting increased expression of genes associated with neutrophils in tumor stroma of SR versus FI tumors (n=22). C) Representative images of IHC depicting accumulation of neutrophils in the tumor stroma of SR versus FI tumors. n=19. Scale is 100µm.

Supplemental Figure 7



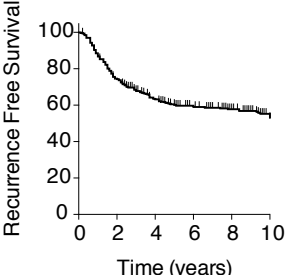
Supplemental Figure 7. A subset of tumors with CD8⁺ T cell accumulation in the tumor stroma display distinct TME with elevated levels of IL-17-producing cells and neutrophils. A) Quantification of IL-17-producing cell density across all SR and FI tumors (n=22). $P = 0.21$. B-C) CD4⁻ (B) and CD4⁺ (C) IL-17-producing cell density across SR and FI tumors (n=10; 5 patients with the lowest and the highest epiCD8 respectively for SR and FI). D) Percentage of CD4⁺ IL-17-producing cell density over the total IL-17-producing cell density across SR and FI tumors (n=10; 5 patients with the lowest and the highest epiCD8 respectively for SR and FI). E-F) CD4⁻ (E) and CD4⁺ (F) IL-17-producing cell density across all SR and FI tumors (n=22). G) Percentage of CD4⁺ IL-17-producing cell density over the total IL-17-producing cell density across all SR and FI tumors (n=22). H) Quantification of neutrophil density across all SR and FI tumors (n=19). $P = 0.27$. Mann-Whitney test. Error bars, mean±SEM.

Supplemental Figure 8



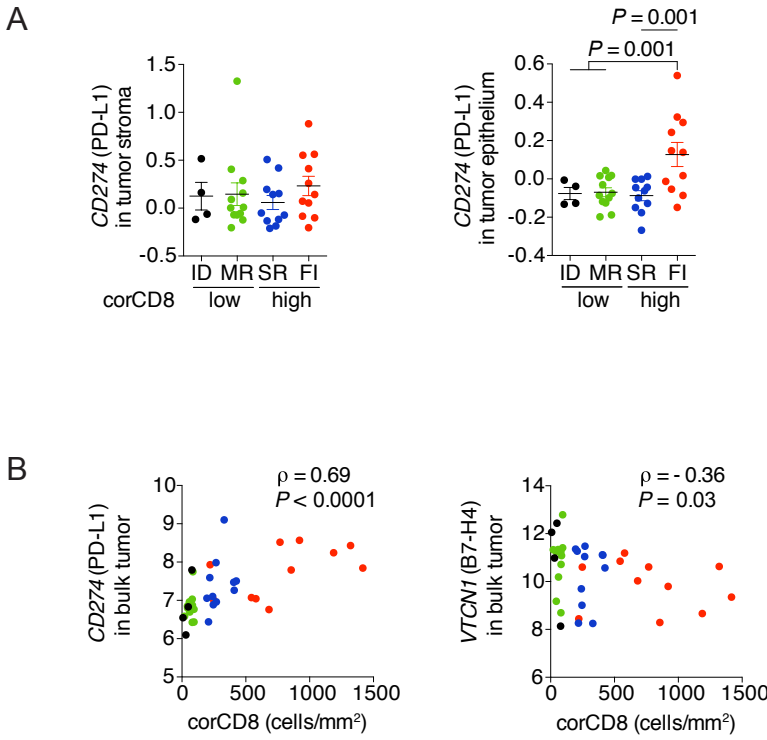
Supplemental Figure 8. A) Representative image of MHC I IHC in all tumors. For Immune desert (ID) and Margin restricted (MR), images are ordered by marCD8 (from left to right and from up to down). For Stroma restricted (SR) and Fully inflamed (FI), patients are ordered by epiCD8. n=36. Images are 500µm by 500µm. B) Quantification of MHC I expression by tumor epithelial cells in all subtypes (left) and comparing FI versus non FI tumors (right). n=36. Fischer exact test. C) Quantification of IL-17 producing cells and neutrophil density per tumor. Tumors are ordered by epiCD8 showing that the SR tumor with the lowest epiCD8 (SR tumor on the very left, arrowhead) has no accumulation of IL-17 producing cells nor neutrophils (n=10). ID, Immune desert. MR, Margin restricted. SR, Stroma restricted. FI, Fully inflamed.

Supplemental Figure 9



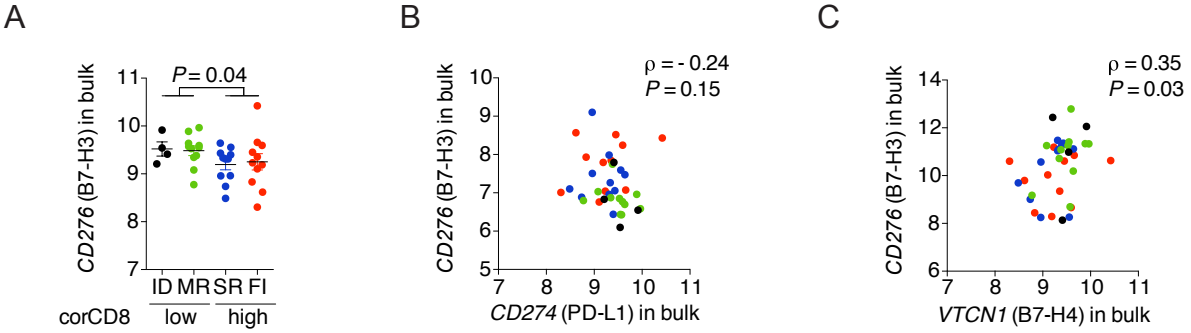
Supplemental Figure 9. Recurrence free survival curve of the Rody *et al.* TNBC gene expression dataset (n=576). This external dataset is a compendium of TNBC from a single platform (Affymetrix U133A and U133 Plus 2.0 chips) and includes only samples that were defined as triple negative based on the mRNA expression of ER, PgR, and HER2 status.

Supplemental Figure 10



Supplemental Figure 10. Immune checkpoint expression levels and correlation with corCD8. A) Gene expression level of *CD274* (PD-L1) expression in tumor stroma (left) and epithelium (right) (n=38). Kruskal Wallis. B) *CD274* (PD-L1) expression (left) is positively correlated whereas *VTCN1* (B7-H4) (right) is inversely correlated with corCD8 (n=37). Spearman correlation. Error bars, mean \pm SEM. Black, green, blue and red dots represent ID, MR, SR and FI tumors respectively.

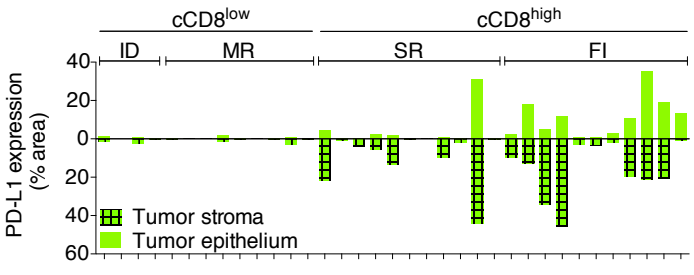
Supplemental Figure 11



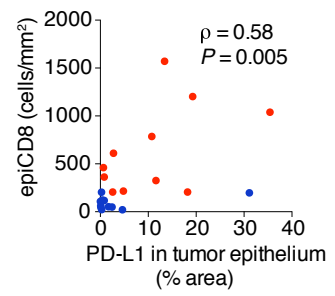
Supplemental Figure 11. TIME TNBC subtypes display distinct expression of immune suppression markers. A) *CD276* (B7-H3) gene expression in bulk tumor (n=37) show increased expression in ID and MR compared to SR and FI tumors. Mann-Whitney test. Error bars, mean \pm SEM. B) *CD276* (B7-H3) and *CD274* (PD-L1) gene expression trend towards inverse correlation (n=37). Spearman correlation. C) *CD276* (B7-H3) and *VTCN1* (B7-H4) show positive correlation in bulk tumor (n=37). Spearman correlation. Black, green, blue and red dots represent ID, MR, SR and FI tumors respectively. ID, Immune desert. MR, Margin restricted. SR, Stroma restricted. FI, Fully inflamed.

Supplemental Figure 12

A

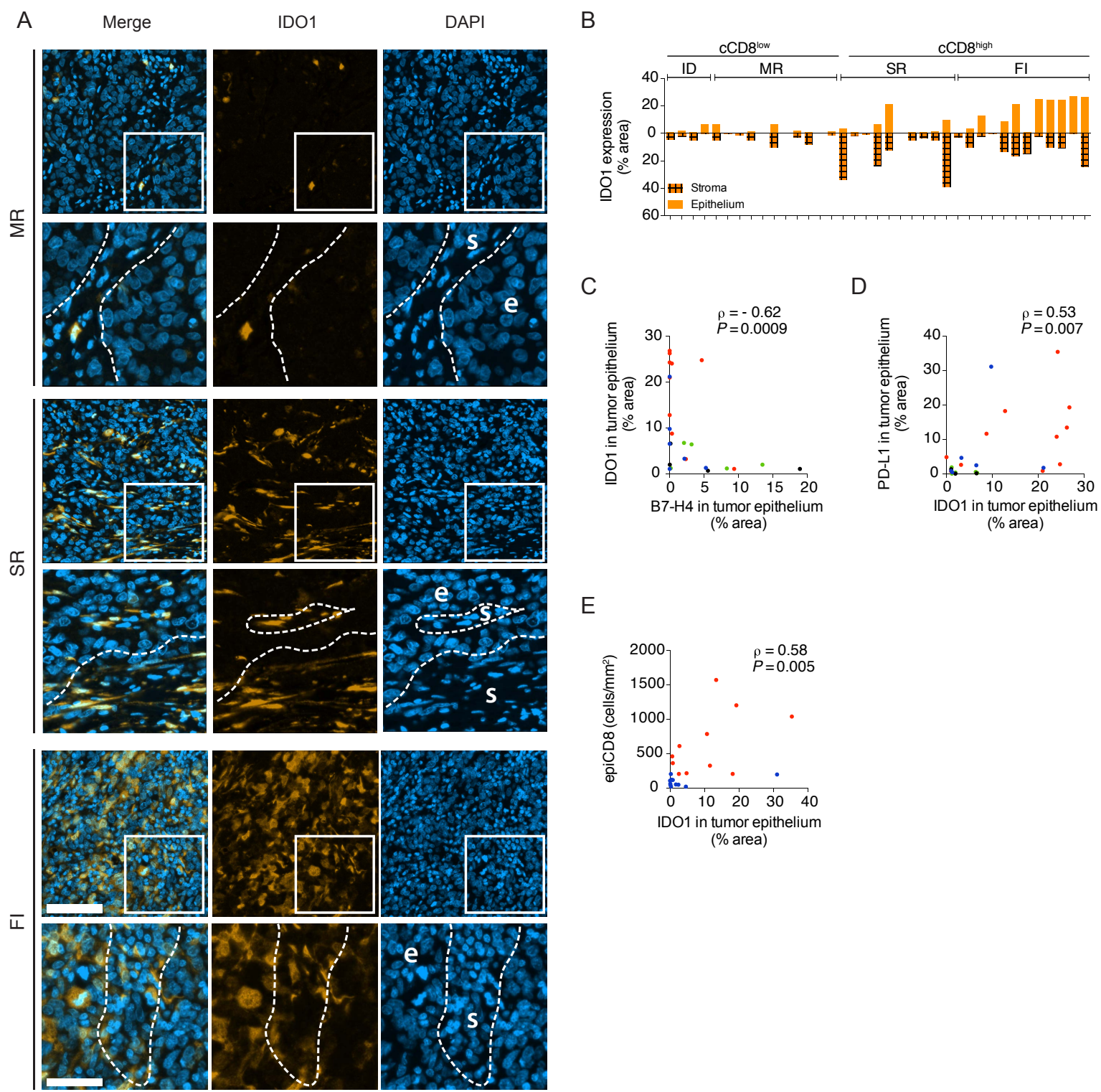


B



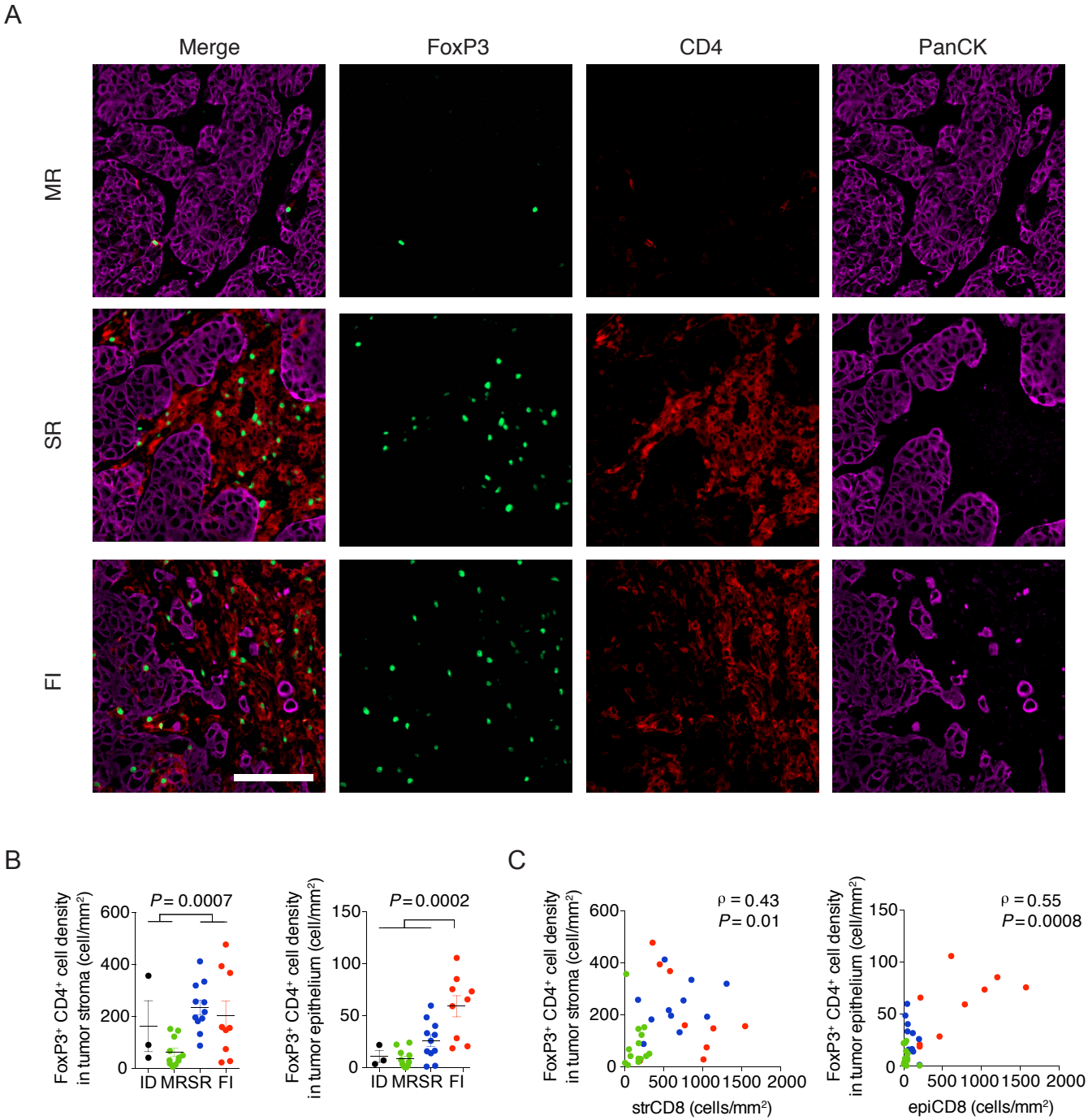
Supplemental Figure 12. TIME TNBC subtypes display distinct localization of PD-L1. A) Quantification of staining in the tumor epithelial (plain green) and stromal (striped green) compartment for PD-L1 per patient (n=35). B) PD-L1 quantification in tumor epithelium is correlated with epiCD8 in corCD8^{high} tumors (n=22, SR and FI). Spearman correlation. Mann-Whitney test. Blue and red dots represent SR and FI tumors respectively.

Supplemental Figure 13



Supplemental Figure 13. TIME TNBC subtypes display distinct expression and localization of IDO1. A) Representative images of IDO1 (orange) and DAPI (blue) IHC stained sections. Dotted line indicates limit of tumor epithelium (e) and stroma (s). Scale is 100µm and 200µm for the image and zoom respectively. B) Quantification of staining in the tumor epithelial (plain) and stromal (stripped) compartment for IDO1 per patient (n=35). C) IDO1 and B7-H4 quantifications on IHC show inverse correlation in the tumor epithelium compartment. This excludes tumors with <1% of stained epithelium for both markers. (n=35). D) IDO1 and PD-L1 quantifications on IHC show positive correlation in the tumor epithelium compartment. This excludes tumors with <1% of stained epithelium for both markers. (n=35). E) IDO1 quantification in tumor epithelium is correlated with epiCD8 in corCD8^{high} tumors (n=22, SR and FI). Spearman correlation. Mann-Whitney test. Black, green, blue and red dots represent ID, MR, SR and FI tumors respectively.

Supplemental Figure 14



Supplemental Figure 14. FoxP3⁺ CD4⁺ cells follow the same spatial distribution pattern of the CD8⁺ T cells. A) Representative images showing FoxP3⁺ CD4⁺ cells spatial distribution in MR, SR and FI tumors. PanCK (pink) staining identifies tumor cells. n=34. Scale is 100µm. B) Quantification of FoxP3⁺ CD4⁺ cells in tumor stroma and tumor epithelium (n=34). Mann-Whitney test. Error bars, mean±SEM. C) Correlation of the FoxP3⁺ CD4⁺ cells density in tumor stroma and tumor epithelium with strCD8 and epiCD8, respectively (n=34). Black, green, blue and red dots represent ID, MR, SR and FI tumors respectively.

Supplemental Table 1

	ID (4)	MR (12)	SR (11)	FI (11)	P value
Age (years, mean \pm SD)	64 \pm 18	52 \pm 12	62 \pm 16	56 \pm 13	0.28
Age (range)	(51-90)	(34-73)	(40-89)	(35-79)	
Tumor size (mm, mean \pm SD)	17 \pm 11	22 \pm 14	18 \pm 5	26 \pm 14	0.65
Ki67 (% , mean \pm SD)	60 \pm 19	62 \pm 19	57 \pm 20	55 \pm 21	0.89
Histological subtype					
IDC-NOS	4	12	11	11	NA
Nodal Status					
positive	0	6	6	2	0,2378
negative	3	3	3	7	
unknown	1	3	2	2	
Breast Cancer Subtype					
Basal	3	9	10	10	0,4973
Other	1	3	1	1	
Grade					
II	1	2	0	0	0,1733
III	3	10	11	11	
Menopausal status					
pre	1	5	4	3	0,7679
peri	0	0	0	2	
surgical/post	3	7	7	6	
Surgery					
mastectomy	3	7	5	4	0,5746
lumpectomy	1	5	6	7	
Adjuvant radiotherapy					
yes	2	7	9	9	0,4953
no	1	4	2	2	
unknown	1	1	0	0	
Adjuvant chemotherapy					
yes	2	10	8	8	0,5878
no	1	1	3	2	
unknown	1	1	0	1	

Supplemental Table 1. Patient characteristics and clinicopathological features of TNBCs in our LCM cohort (n=38 tumors). Main patient characteristics and clinicopathological features of triple negative breast cancer in our LCM cohort (n=38 tumors) for the entire cohort and for the groups defined by CD8⁺ T cell localization (ID, MR, SR and FI). ID, Immune desert ; MR, Margin restricted ; SR, stroma restricted ; FI, Fully inflamed. Samples were collected from patients undergoing breast surgeries at the McGill University Health Centre (MUHC) between 1999 and 2012. For this study, samples were selected according to the following criteria: therapy-naïve at time of surgical excision, clinically documented lack of expression/amplification of ER, PR and HER2 and a histological subtype of invasive ductal carcinoma (not otherwise specified) (IDC (NOS)). For tumor size, age Ki67, significance was assessed by one-way ANOVA. Categorical factors (Nodal Status, Breast Cancer Subtype, Grade, Menopausal status, Surgery, Adjuvant radiotherapy, Adjuvant Chemotherapy, disease free survival and overall survival) are represented as number of tumors positive for each category and significance was assessed by Fischer exact test.